Article

Neuron

HCN2 Channels in Cholinergic Interneurons of Nucleus Accumbens Shell Regulate Depressive Behaviors

Graphical Abstract

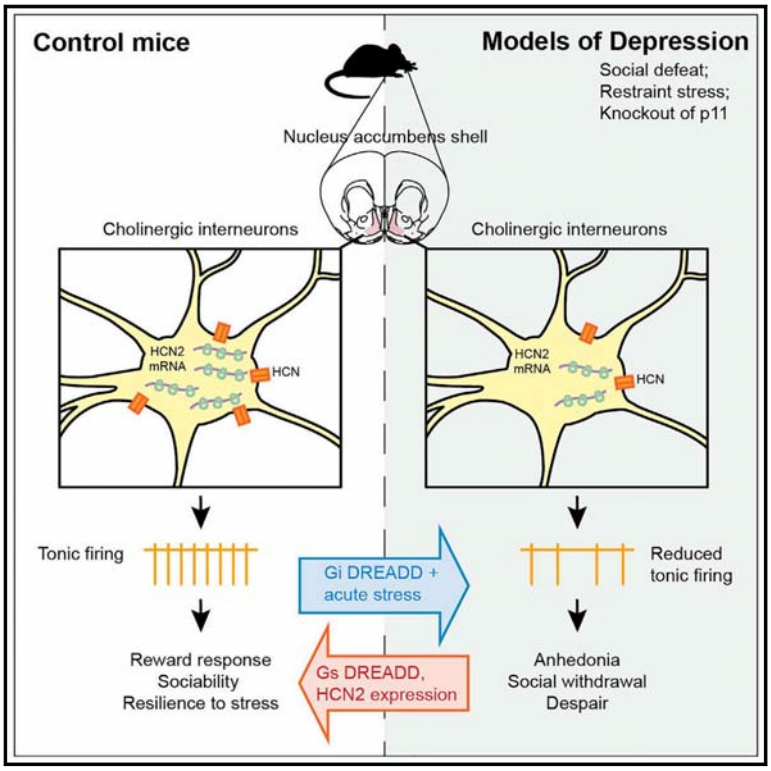

Highlights

- ChI activity is decreased in NAc shell in mouse models of depression
- Inhibition of ChIs renders naive mice susceptible to stress
- Dysfunction of HCN2 channels underlies reduced ChI activity in depressive mice
- Enhancing ChI activity by chemogenetics or HCN2 overexpression rescues depression

Authors

Jia Cheng, Gali Umschweif, Jenny Leung, Yotam Sagi, Paul Greengard

Correspondence

ysagi@rockefeller.edu (Y.S.), greengard@rockefeller.edu (P.G.)

In Brief

Cheng et al. show that decreased expression and function of HCN2 channels cause reduced ChI tonic activity in NAc shell that leads to depressive phenotypes. Targeting HCN2 channels to enhance ChI activity is sufficient to rescue depression.

Cheng et al., 2019, Neuron *101*, 1–11
February 20, 2019
https://doi.org/10.1016/j.neuron.2018.12.018

CellPress

Please cite this article in press as: Cheng et al., HCN2 Channels in Cholinergic Interneurons of Nucleus Accumbens Shell Regulate Depressive Behaviors, Neuron (2018), https://doi.org/10.1016/j.neuron.2018.12.018

Neuron
Article

HCN2 Channels in Cholinergic Interneurons of Nucleus Accumbens Shell Regulate Depressive Behaviors

Jia Cheng,[1] Gali Umschweif,[1] Jenny Leung,[1] Yotam Sagi,[1,*] and Paul Greengard[1,2,*]
[1]Laboratory of Molecular and Cellular Neuroscience, The Rockefeller University, New York, NY 10065, USA
[2]Lead Contact
*Correspondence: ysagi@rockefeller.edu (Y.S.), greengard@rockefeller.edu (P.G.)
https://doi.org/10.1016/j.neuron.2018.12.018

SUMMARY

Cholinergic interneurons (ChIs) in the nucleus accumbens (NAc) have been implicated in drug addiction, reward, and mood disorders. However, the physiological role of ChIs in depression has not been characterized. Here, we show that the tonic firing rate of ChIs in NAc shell is reduced in chronic stress mouse models and in a genetic mouse model of depression. Chemogenetic inhibition of NAc ChIs renders naive mice susceptible to stress, whereas enhancement of ChI activity reverses depressive phenotypes. As a component of the molecular mechanism, we found that the expression and function of the hyperpolarization-activated cyclic nucleotide-gated channel 2 (HCN2) are decreased in ChIs of NAc shell in depressed mice. Overexpression of HCN2 channels in ChIs enhances cell activity and is sufficient to rescue depressive phenotypes. These data suggest that enhancement of HCN2 channel activity in NAc ChIs is a feasible approach for the development of a new class of antidepressants.

INTRODUCTION

Depression is a highly heterogeneous disorder. The understanding of the etiology of depression is limited and the clinical treatment is inadequate (Belmaker and Agam, 2008). Multiple lines of study have indicated that depression is attributable to genetic factors with a heritability of ~35% (Geschwind and Flint, 2015; Sullivan et al., 2000), and environmental factors such as stressors (Nestler et al., 2002). Accordingly, it is necessary to investigate the common mechanisms underlying the pathophysiology of depression by using multiple animal models that have been developed to capture the diversity of depressive symptoms and causes (Akil et al., 2018).

As a key brain region in the reward circuit, the nucleus accumbens (NAc) is divided into two subregions, shell and core, that have distinct anatomical and functional features (Brog et al., 1993; Meredith et al., 2008; Voorn et al., 2004). NAc shell may encode different aspects of behaviors compared to the core. For example, social-isolation-induced anxiety (Wallace et al., 2009) and reinstatement of drug seeking (Cruz et al., 2014) are mediated by NAc shell; NAc shell is a key node in the circuit for neuropathic pain (Ren et al., 2016); and dopamine release is preferentially elevated in NAc shell in response to addictive drug (Pontieri et al., 1995). The specific role of NAc shell and core in the pathophysiology of depression, however, is poorly understood.

Although composing one percent of the local neuronal population, cholinergic interneurons (ChIs) provide a major source of acetylcholine in the NAc and play a dominant control role in regulating NAc activity and function (Witten et al., 2010; Zhou et al., 2002). Recent studies have reported that NAc ChIs are involved in addictive drug-associated learning (Lee et al., 2016; Witten et al., 2010) and in the motivation for food satiety (Stouffer et al., 2015). NAc ChIs have also been implicated in depression-like behaviors in rodents (Warner-Schmidt et al., 2012). Here, we used genetic and stress-induced models of depression to examine the changes in the tonic activity of ChIs in the core and shell of the NAc. By modulating ChI activity, we revealed that ChIs bi-directionally regulate affective states in rodents.

RESULTS

ChI Activity Is Reduced in NAc Shell in Mouse Models of Depression

To investigate the role of NAc ChIs in depression, we used three well-established mouse models of depression: chronic social defeat stress (SDS) mice, chronic restraint stress (RS) mice, and p11 conditional knockout (cKO) mice (Akil et al., 2018; Oh et al., 2013; Warner-Schmidt et al., 2012). To visualize ChIs, ChAT-eGFP mice were used for stress mouse models or crossed with p11 cKO mice. Immunostaining and electrophysiology confirmed that eGFP positive cells were co-localized with the ChI marker choline acetyltransferase (ChAT) and exhibited physiological characteristics of ChIs (Figures S1A and S1B). Accordingly, all subsequent electrophysiological recordings were performed on eGFP-positive cells to study neuronal activities of ChIs in NAc shell and core (Figures 1A and 1B).

The chronic SDS mice are a stress-induced mouse model that reliably exhibits an array of depression-like behaviors (Golden et al., 2011). Mice that underwent 10-day chronic SDS were separated into susceptible or resilient groups based on their social interaction (SI) ratio and the time spent in the interaction zone in the presence of aggressors. Control mice, on the other hand,

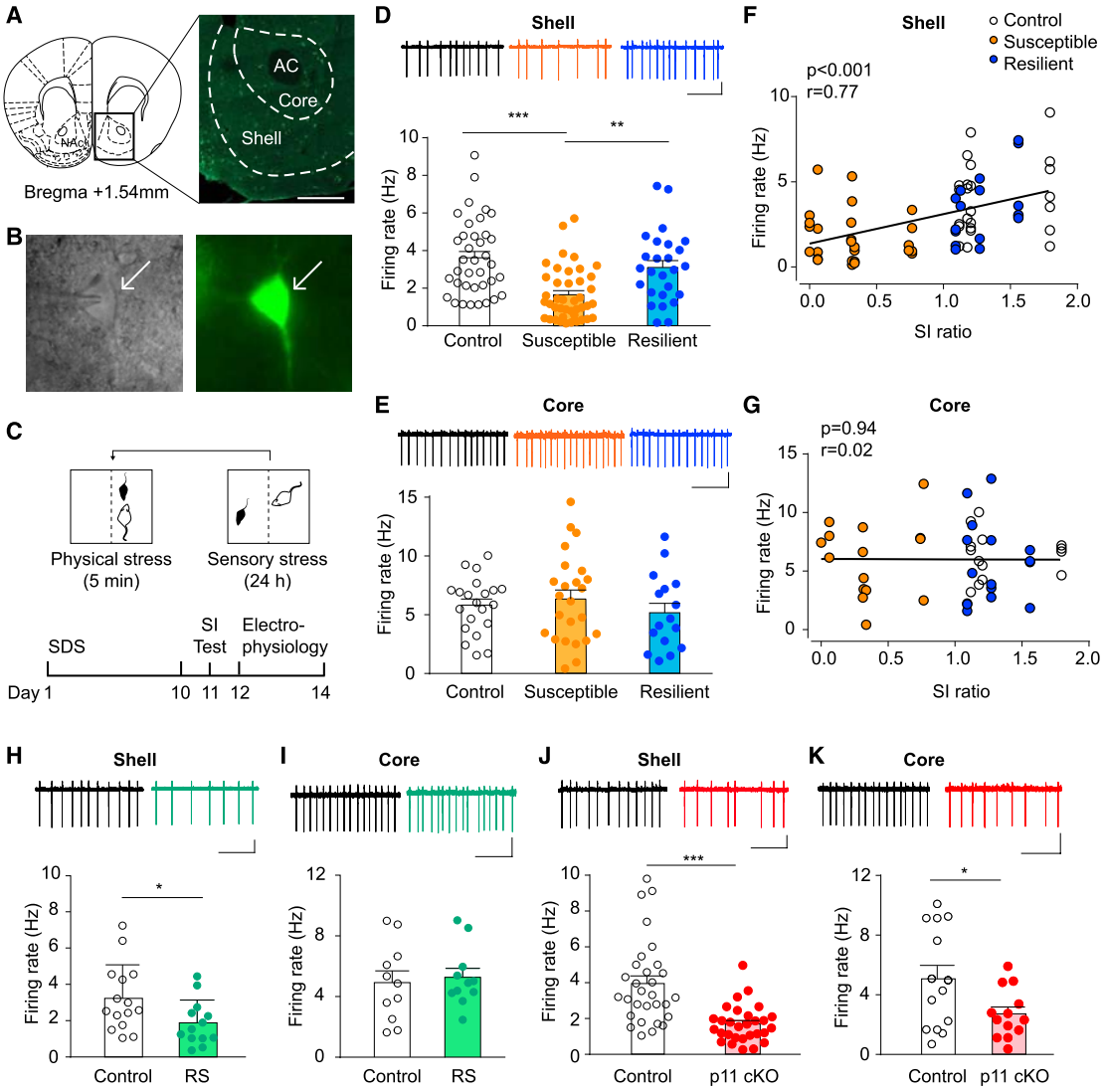

Figure 1. Tonic Firing Rate of ChIs Is Diminished in Mouse Models of Depression

(A) Schematic of a coronal brain section at the level of nucleus accumbens (NAc). Inset: NAc shell and core in a brain slice from ChAT-eGFP mice. Scale bar, 500 μm. AC, anterior commissure.

(B) Photomicrograph of an eGFP$^+$ ChI (white arrow) under electrophysiological recording.

(C) Schematic of social defeat stress (SDS) and experimental timeline. SI, social interaction.

(D and E) Representative traces and summary graphs showing the firing rate of ChIs in NAc shell (D, one-way ANOVA, $p < 0.001$) and NAc core (E, one-way ANOVA, $p = 0.53$) in SDS mice. n = 16–42 cells from 6–11 mice per group.

(F and G) SI ratio correlates with ChI firing rate in NAc shell (F, Pearson correlation, $p < 0.001$, $r = 0.77$), but not in NAc core (G, Pearson correlation, $p = 0.94$, $r = 0.02$) in SDS mice. n = 24 cells from 4 control mice, 28 cells from 7 susceptible mice, 17 cells from 4 resilient mice.

(H and I) Representative traces and summary graphs of ChI firing rate in NAc shell (H) and core (I) in chronic restraint stressed (RS) mice. Unpaired t test. n = 11–15 cells from 4–5 mice per group.

(J and K) Representative traces and summary graphs of ChI firing rate in NAc shell (J) and core (K) in p11 cKO mice. Unpaired t test. n = 13–30 cells from 5–9 mice per group.

Scale bar for (D), (E), and (H)–(K), 20 pA, 1 s. Data are represented as means ± SEM. *$p < 0.05$, **$p < 0.01$, ***$p < 0.001$.

See also Figures S1 and S2.

were housed in pairs during the defeat sessions with no physical or sensory contact with aggressor mice (Figures 1C and S1C–S1F). SDS mice were further examined in the social approach (SA) test, a commonly used test for sociability (Moy et al., 2004). Consistently, susceptible mice exhibited social avoidance while control and resilient mice exhibited strong SI in the SA test (Figures S1G–S1J). SA preference index correlated with SI ratio in the SDS mice (Figure S1K).

Cell-attached voltage clamping was next performed to produce reliable, long-lasting, and stable recording of ChI firing rates in SDS mice (Bennett et al., 2000). ChIs are spontaneous firing neurons *in vitro* and *in vivo*. Tonic firing rates of ChIs have been reported ranging from 0.3 to 10 Hz previously (Witten et al., 2010; Virk et al., 2016). Strikingly, we found that the tonic firing rate of ChIs was selectively diminished in NAc shell in susceptible mice compared to that in control mice (Figure 1D). The firing rate of ChIs in NAc shell was unchanged in resilient mice (Figure 1D). On the other hand, the firing rate of ChIs in NAc core remained unaltered in the susceptible mice and resilient mice compared to control mice (Figure 1E). We also revealed that ChI firing rate in NAc shell, but not NAc core, correlated with SI ratio (Figures 1F and 1G).

To further confirm the region-specific alteration of ChI activity in depressed mice, we used the chronic RS mouse model. RS is a mild stress that induces short-term, but not long-term depressive phenotypes in rodents, including diminished sucrose consumption in the sucrose preference test (SPT), reduced SI in the SA test, increased immobility in the forced swim test (FST), and in the tail suspension test (TST), unaltered total exploration time in the SA, and unaltered distance traveled in the open-field (OF) test (Figure S2). In accordance with the SDS model, the tonic firing rate of ChIs in the RS mice was selectively reduced in NAc shell, but not in NAc core (Figures 1H and 1I).

Taking advantage of a genetic mouse model of depression, we used p11 cKO mice to examine the neuronal activity of ChIs in NAc shell and core. p11 (S100A10) is a small intracellular protein involved in the pathophysiology of depression and the action of antidepressants (Alexander et al., 2010; Oh et al., 2013; Svenningsson et al., 2006, 2013). The deletion of p11 from NAc ChIs has been shown to induce anhedonia and behavioral despair in mice (Warner-Schmidt et al., 2012). Here, we found that the tonic firing rate of ChIs was significantly reduced in both NAc shell and core in p11 cKO mice, indicating a p11-dependent genetic modulation on the neuronal activity of ChIs regardless of cell localization (Figures 1J and 1K).

Combined with our electrophysiology results from stress mouse models and the genetic mouse model of depression, we suggest that the diminished ChI activity in NAc shell is a common feature among these models of depression.

Chemogenetic Inhibition of NAc ChIs Combined with an Acute Stress Induces Depressive Behaviors

To investigate whether ChIs play a causal role in depression, we suppressed ChI activity *in vivo* by using the designer receptors exclusively activated by designer drugs (DREADDs), a chemogenetic technology to manipulate neuronal activity in a cell-type-specific manner (Roth, 2016).

Adeno-associated viruses (AAVs) expressing the Cre-dependent inhibitory DREADD (AAV2-hSyn-DIO-hM4D(Gi)-mCherry) or a control vector (AAV2-hSyn-DIO-mCherry) were bilaterally injected into the NAc of ChAT-Cre mice (Figure 2A). To ensure a high percentage of ChIs expressing DREADD receptors, 1 μL AAV was injected into the region of interest. We confirmed that the virus infected ChIs in both NAc shell and core (Figure 2B). Images obtained by confocal microscopy showed the selective and restricted expression of DREADD AAVs in the ChIs from ChAT-Cre::ChAT-eGFP mice (Figure 2C). Next, we performed electrophysiological recordings in NAc slices to validate the inhibitory effect of the Gi (hM4D) DREADD on ChI activity (Figure S3A). Bath application of the DREADD ligand, clozapine N-oxide (CNO), had no effect on the firing rate of ChIs expressing mCherry, but significantly inhibited the ChIs expressing Gi DREADD (Figure S3B). DREADD receptors or CNO itself did not change the basal firing rate of ChIs (Figure S3B).

Next, we performed a battery of depression-related tasks to examine behavioral consequences in ChAT-Cre mice expressing DREADDs (Figure S3C). We found that acute injection of CNO remarkably suppressed the sucrose consumption and SI in mice expressing Gi DREADD in the NAc ChIs (Figures S3D and S3F). Inhibition of the NAc ChIs did not change the total exploration time in the SA test, immobility in the FST and TST, and the locomotor activity in the OF (Figures S3E and S3G–S3I). These data suggest that inhibition of ChIs in the NAc play a dominant role in inducing anhedonia and social avoidance in rodents. The mCherry virus or administration of CNO had no effect on the depression-like behaviors (Figures S3D–S3I), which excluded off-target effects (Gomez et al., 2017).

Previous studies have shown that subthreshold SDS (SSDS) has no behavioral effect in wild-type mice. Only mice that are vulnerable to acute stress develop depressive phenotypes after SSDS (Golden et al., 2011; Chaudhury et al., 2013). Here, we showed that the combination of SSDS and inhibition of NAc ChIs by Gi DREADD induced depressive phenotypes in mice, as indicated by the reduction in SI and sucrose preference and increase in the immobility in the FST and TST but caused no change in locomotion (Figures 2D–2J). Taken together, these data suggest that inhibition of NAc ChIs promotes susceptibility to depression in mice.

Enhancement of ChI Activity Reverses Depressive Behaviors

Given that diminished tonic firing of NAc ChIs was a common characteristic in depressed mice, we hypothesized that enhancing NAc ChI activity reverses the behavioral deficits in mouse models of depression. To selectively activate NAc ChIs *in vivo*, we bilaterally injected AAVs expressing the excitatory DREADD (AAV2-hSyn-DIO-rM3D(Gs)-mCherry) into the NAc of ChAT-Cre mice (Figures 3A and S4A). Cell-attached current-clamp recordings confirmed that the application of CNO on the NAc slices effectively increased the firing rate of ChIs expressing Gs(rM3D) DREADD (Figure S4B).

Next, we injected Gs DREADD virus to the NAc of SDS mice and p11 cKO mice. RS mice were not used due to the fact that depressive phenotypes in RS mice failed to last for 3 weeks (Figure S2). In the SDS model, susceptible mice were selected after 10-day SDS using the SI test. Mice were then stereotaxically injected with AAVs expressing either mCherry or Gs DREADD. They were allowed 3 weeks to fully express DREADD receptors before the SI test with either a single dose or 14-day injections of CNO (Figure 3B). Acute activation of Gs DREADD failed to modulate behavioral phenotypes in susceptible mice. In contrast, chronic activation of Gs DREADD by 14-day injection of CNO reversed social avoidance in a subset of susceptible mice (Figure 3C). This is possibly due to the individual differences among

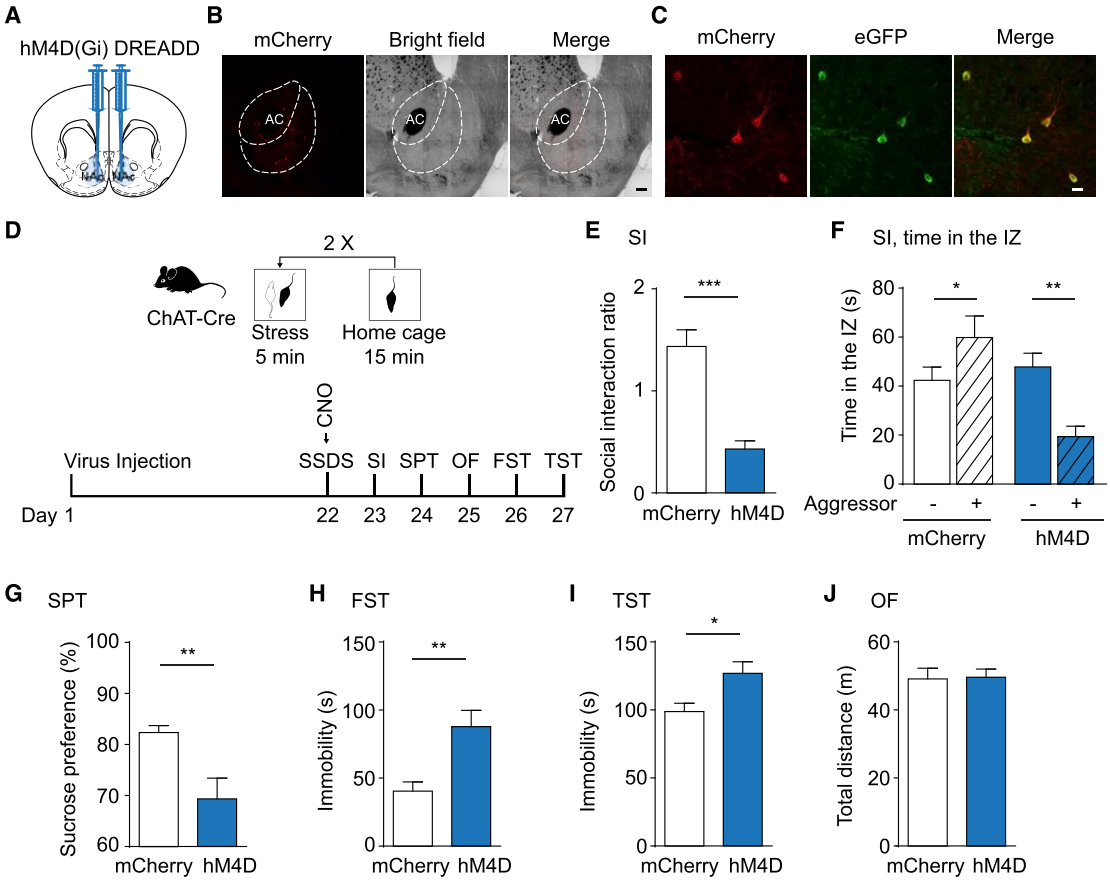

Figure 2. Chemogenetic Inhibition of ChIs Renders Mice Susceptible to Depression

(A) Schematic of virus injection into the NAc of ChAT-Cre mice.

(B) Representative confocal images showing a restrictive expression of DREADD virus (mCherry, red) in the NAc. Scale bar, 500 μM.

(C) Images showing the co-localization of DREADD (mCherry, red) with ChIs (eGFP, green). Scale bar, 20 μm. mCherry-expressing $eGFP^+$ cells are 83.0% ± 8.0% of total $eGFP^+$ neurons in the NAc. No expression of mCherry is in $eGFP^-$ neurons (2–3 sections per mouse; n = 3 mice).

(D) Schematic of experimental design.

(E–J) Behavioral tests of mice expressing mCherry or hM4D DREADD after subthreshold SDS. SI test (E and F), sucrose preference test (G), forced swim test (H), tail suspension test (I), and open-field test (J). Unpaired t test for (E) and (G)–(J); two-way repeated-measures ANOVA for (F) (interaction, $p < 0.001$). n = 10 mCherry mice, n = 12 hM4D mice.

Data are presented as means ± SEM. *$p < 0.05$, **$p < 0.01$, ***$p < 0.001$.

See also Figure S3.

animals such as gene expression profile or brain regions that are dysfunctional during SDS. Moreover, the amount of time susceptible mice spent in the interaction zone when an aggressor was present was significantly increased by chronic activation of Gs DREADD (Figure 3D). Chronic CNO treatment had no effect on either behaviors or neuronal activity in susceptible mice expressing the control virus, excluding off-targets effects (Gomez et al., 2017).

To investigate the physiological regulation on ChIs by chronic activation of Gs DREADD, we assessed the ChI firing rate from mice treated with CNO for 14 days. The mCherry fluorescence, an indicator for the expression of Gs DREADD, maintained strong in the ChIs after chronic CNO treatment (Figure 3E). Importantly, electrophysiological recordings showed that basal neural activity was significantly enhanced in Gs DREADD-positive ChIs relative to mCherry ChIs after 14-day CNO treatment in susceptible mice (Figure 3F). Gs DREADD maintained functional as reflected by the response of ChIs to a bath application of CNO (Figure 3F). To further confirm the enhanced ChI activity by chronic activation of Gs DREADD, we tested the stress-naive mice. In line with the results in susceptible mice, 14-day activation of Gs DREADD significantly enhanced basal ChI firing rate in stress-naive mice (Figure S4C), while the response of Gs DREADD to CNO was maintained in the ChIs (Figure S4D).

Consistent with our findings in the SDS model, enhancement of ChI firing rate by Gs DREADD profoundly reversed depressive behaviors in p11 cKO mice, as reflected in elevated sucrose consumption and SI, and reduced immobility in the FST and TST (Figures 3G–3K). Gs DREADD had no effect on total exploration time in SA and locomotor activity in OF (Figures 3I and 3L). These

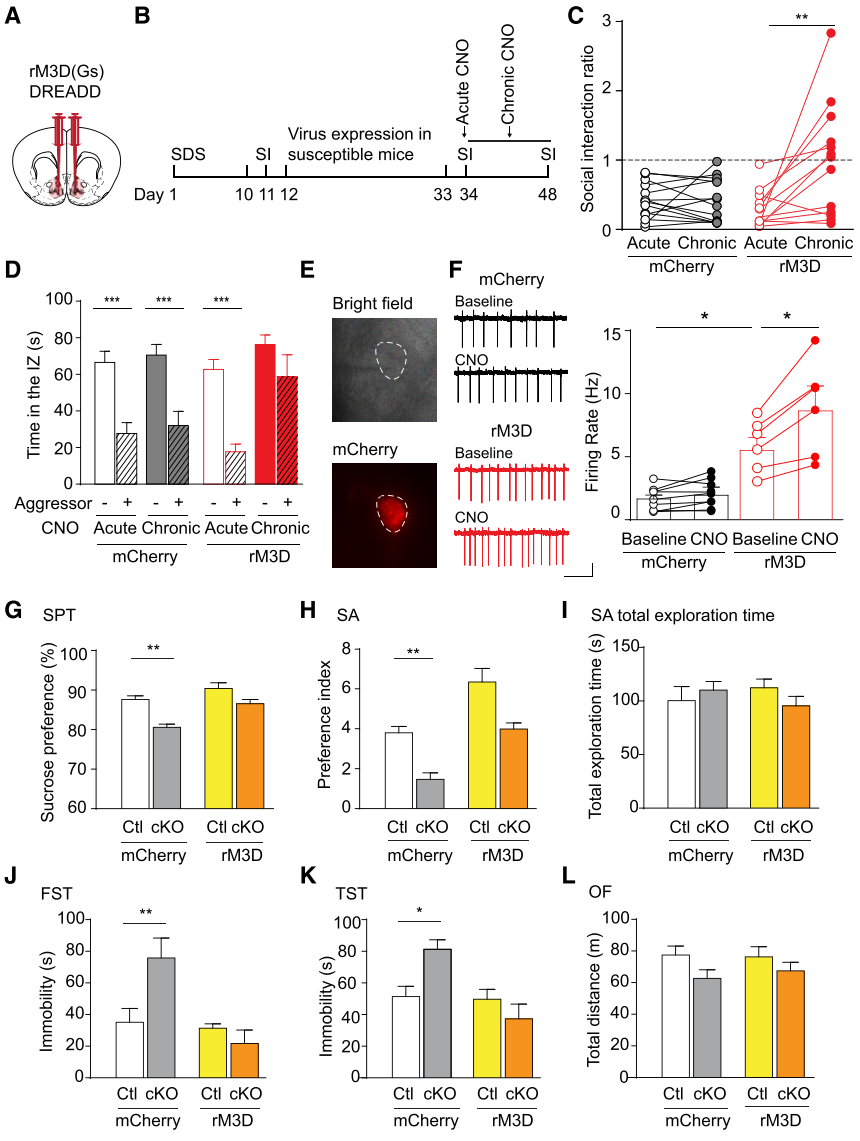

Figure 3. Enhancing ChI Activity Reverses Depressive Behaviors

(A) Schematic of virus injection into the NAc of ChAT-Cre mice.

(B) Timeline of experimental design.

(C) SI ratio of susceptible mice expressing mCherry or rM3D DREADD treated with a single (acute) or 14-day (chronic) injection of CNO (1 mg/kg, i.p.). Two-way repeated-measures ANOVA (interaction, $p = 0.01$). n = 14 mCherry mice, n = 13 rM3D mice.

(D) Time spent in the interaction zone of susceptible mice expressing mCherry or rM3D DREADD in the absence or presence of aggressors with an acute or chronic CNO treatment. Two-way repeated-measures ANOVA (interaction, $p = 0.01$).

(E) Photomicrograph of electrophysiological recordings on an mCherry$^+$ ChI from a mouse that had undergone chronic CNO treatment.

(F) Representative traces and a summary plot showing the firing rate of ChIs from chronic CNO-treated susceptible mice expressing mCherry or rM3D DREADD virus. ChI firing rate is recorded before and after a bath application of CNO (1 μM). Two-way repeated-measures ANOVA (interaction, $p = 0.03$). n = 8 mCherry cells, 6 rM3D cells, 3 mice per group. Scale bar, 20 pA, 1 s.

(G–L) Behavioral tests on control (Ctl) and p11 cKO mice expressing mCherry or rM3D DREADD after a single injection of CNO. Two-way ANOVA. n = 9–14 mice per group.

(G) Sucrose preference test (interaction, $p = 0.17$; genotype, $p < 0.01$; DREADD, $p < 0.001$).

(H) Social approach preference index (interaction, $p = 0.14$; genotype, $p < 0.01$; DREADD, $p < 0.001$).

(I) Social approach total exploration time (interaction, $p = 0.19$; genotype, $p = 0.73$; DREADD, $p = 0.89$).

(J) Forced swim test (interaction, $p < 0.01$; genotype, $p = 0.07$; DREADD, $p < 0.01$).

(K) Tail suspension test (interaction, $p < 0.01$; genotype, $p = 0.22$; DREADD, $p < 0.01$).

(L) Open-field test (interaction, $p = 0.61$; genotype, $p = 0.06$; DREADD, $p = 0.75$).

Data are presented as means ± SEM. $^*p < 0.05$. $^{**}p < 0.01$, $^{***}p < 0.001$.

See also Figure S4.

behavioral results indicate that enhancing ChI activity in the NAc effectively reverses depressive behaviors in the p11 cKO mice. Moreover, activation of ChIs by Gs DREADD was efficient to modulate sucrose consumption and SI in control mice (Figures 3G and 3H), suggesting that ChIs play a central role in controlling reward response and sociability.

Reduced *Hcn2* mRNA in Mouse Models of Depression

We next investigated the molecular mechanisms underlying the diminished ChI activity in the stress mouse model and the genetic mouse model of depression. RNA sequencing (RNA-seq) analysis was performed in samples from NAc ChIs. The global changes in gene expression were analyzed. The p11 cKO mice were chosen because the changes in ChI activity were detected in both shell and core of the NAc, suggesting that the gene expression profile in this cellular population is homogeneous throughout the NAc. Because ChIs represent a minor population of NAc cells, we utilized the translating ribosome affinity purification (TRAP) method to isolate polysome-bound RNA only from NAc ChIs (Virk et al., 2016). To this end, ChAT bacterial artificial chromosome translating ribosomes affinity purification (BacTRAP) mice were crossed with p11 cKO mice. The mRNA level was downregulated in 59 genes and upregulated in 54 genes in p11 cKO mice, relative to control mice (Figure 4A; Table S1). The altered genes were categorized into transcription factors, helicase related factors, signaling molecules, and ion channels (Table S2).

Among the ion channels, *Hcn2* showed a lower expression level in ChIs from p11 cKO mice. This gene encodes the hyperpolarization activated cyclic nucleotide-gated (HCN) channel 2, known as a pacemaker channel in maintaining cardiac rhythm (Ludwig et al., 2003) and regulating neuronal activity (Chan

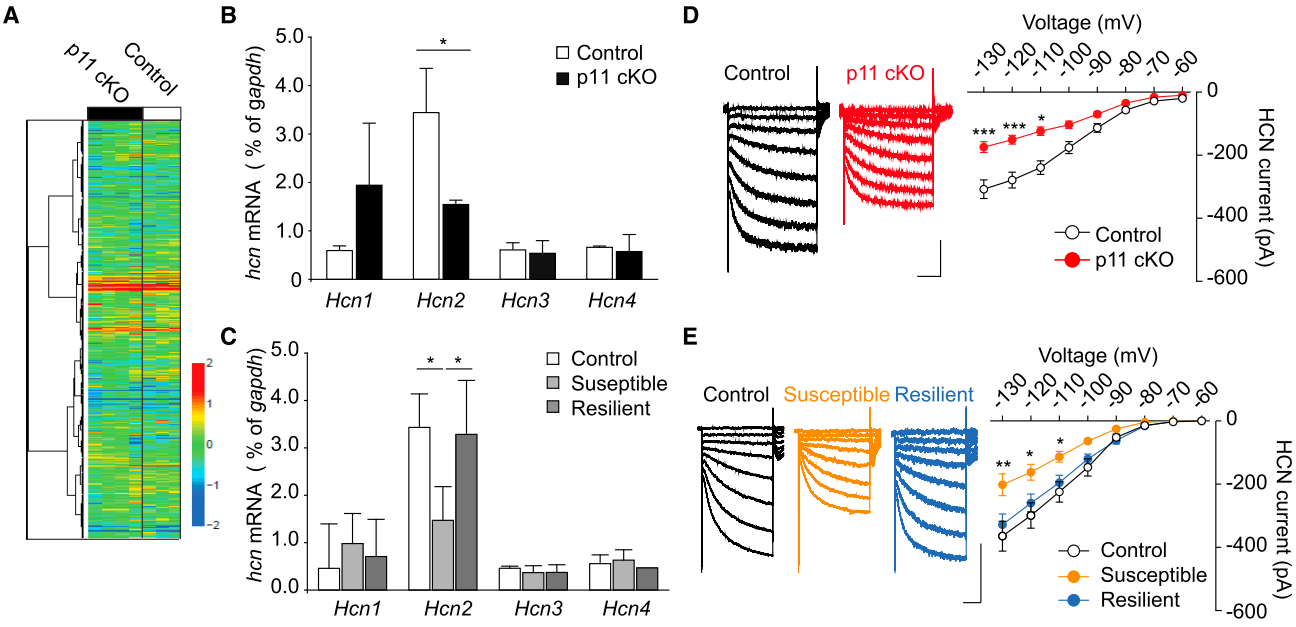

Figure 4. Reduced Expression and Function of HCN2 Channels in ChIs of NAc Shell in Depressive Mice

(A) Heatmap summary of RNA sequencing (RNA-seq) analysis from NAc ChIs between control and p11 cKO mice. n = 3 replicates from 9 control mice and 4 replicates from 12 p11 cKO mice. Note that the vast majority of genes were unchanged in the cKO.

(B and C) Bar graph of the qPCR analysis of *Hcn* gene expression in ChIs from control and p11 cKO mice (B, unpaired t test. n = 3 samples from 9 mice per group) or from SDS mice (C, one-way ANOVA, $p < 0.05$. n = 4 samples from 12 mice per group).

(D and E) Representative traces and current-voltage curve of HCN currents in ChIs of NAc shell in control and p11 cKO mice (D, two-way ANOVA, interaction, $p < 0.001$; genotype, $p < 0.001$; voltage, $p < 0.001$), and in SDS mice (E, two-way ANOVA, interaction, $p < 0.001$; mouse group, $p < 0.001$; voltage, $p < 0.001$). Scale bar, 200 pA, 750 ms. n = 7–14 cells from 3–5 mice per group.

Data are represented as mean ± SD for (B) and (C), as means ± SEM for (D) and (E). *$p < 0.05$, **$p < 0.01$, ***$p < 0.001$.

See also Figure S5 and Tables S1 and S2.

et al., 2004). We corroborated the RNA-seq results by qPCR and found a reduction in the level of *Hcn2* in p11 cKO mice relative to control mice (Figure 4B). In contrast, the expression levels of the *Hcn 1*, *3*, and *4* isoforms were not altered in ChIs in p11 cKO mice (Figure 4B). Interestingly, we found that the level of the *Hcn2* isoform was significantly higher relative to other *Hcn* isoforms in the control mice (Figures 4B and 4C), indicating that HCN2 is the major isoform expressed in the NAc ChIs regulating neuronal activity.

We measured the mRNA level of *Hcn* genes in ChIs from mice subjected to SDS. mRNA was isolated from NAc ChIs from control, susceptible, and resilient ChAT-BacTRAP mice. Consistently, the mRNA level of the *Hcn2* gene in the susceptible mice was lower relative to that either in the control mice or in the resilient mice (Figure 4C). The gene expression level of the *Hcn1*, *3*, and *4* isoforms was not altered in ChIs in the susceptible mice (Figure 4C). Additionally, the expression level for the cholinergic markers *Chat* and *Slc18a3* was not changed in the p11 cKO mice and susceptible mice (Figures S5A and S5B). The expression level of *S100a10*, the gene for p11, was unaltered in the susceptible mice (Figure S5B).

Reduced HCN Function in Depressed Mice

By using electrophysiological approach, we examined whether the function of HCN channels in NAc ChIs was altered in depressed mice. First, immunostaining confirmed the expression of HCN2 channels in the ChIs (Figure S5C). We then employed whole-cell voltage clamping to directly measure HCN channel-mediated currents (I_h) by holding the membrane voltage from −60 to −130 mV in 10-mV steps. In p11 cKO mice, the amplitude of I_h was reduced in ChIs of NAc shell (Figure 4D) and core (Figure S5D), suggesting reduced function of HCN channels. In SDS mice, the HCN currents were selectively reduced in ChIs of NAc shell (Figure 4E), but not of the core (Figure S5E), which is consistent with the selective reduction of ChI firing rate in NAc shell.

The function of HCN channels was further examined by studying the membrane potential of ChIs in response to negative currents (Chan et al., 2011). Negative-current pulses delivered to the ChI soma were more effective in hyperpolarizing the cells in p11 cKO mice than in control mice, as reflected by increased trough potential (Figures 5A and 5B). The hyperpolarization-induced depolarizing sag (Maroso et al., 2016) was significantly reduced in p11 cKO mice (Figures 5A and 5C), which indirectly showed that the HCN channels were dysfunctional. In SDS mice, the presence of negative-current pulses induced more negative voltages in susceptible mice, whereas resilient mice showed a similar voltage-response compared to control mice (Figures 5D and 5E). The sag was significantly reduced in susceptible mice but not resilient mice compared to the control mice (Figure 5F).

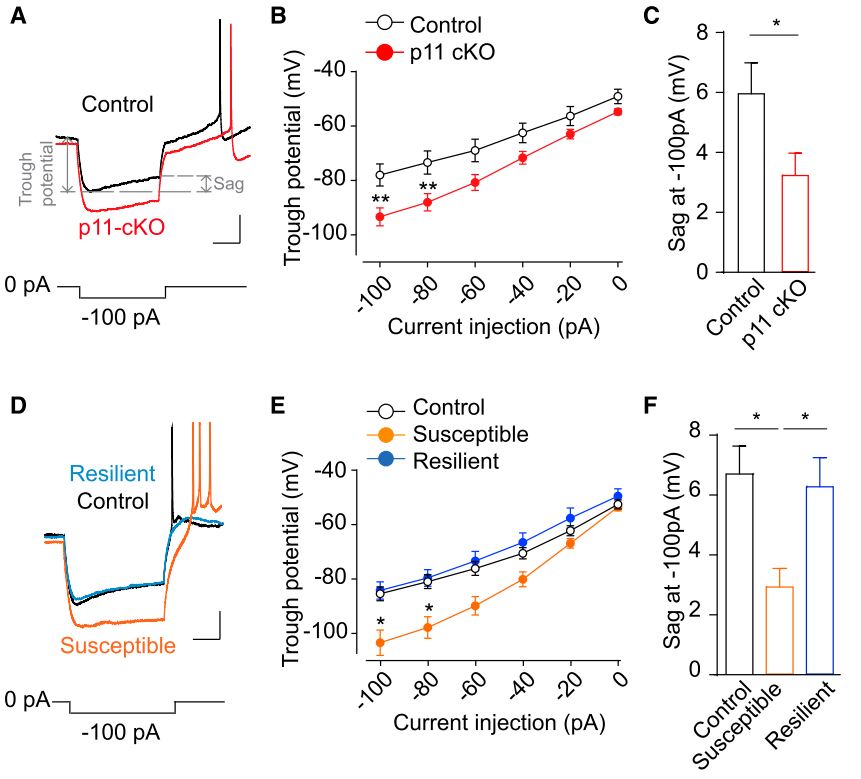

Figure 5. Disrupted HCN2 Function Underlies Decreased ChI Activity in Depressive Mice

(A) Representative traces of ChI membrane response to a series of negative-current injections in control and p11 cKO mice.

(B) Summary graph of trough potential (two-way ANOVA, interaction, $p = 0.52$; genotype, $p < 0.001$; current injection, $p < 0.001$). n = 7–8 cells from 3 mice per group.

(C) Bar graph summarizing the sag at the −100 pA in ChIs (unpaired t test).

(D) Representative traces of ChI membrane response in SDS mice.

(E) Summary graph of trough potential (two-way ANOVA, interaction, $p = 0.16$; mouse group, $p < 0.001$; current injection, $p < 0.001$). n = 7–11 cells from 3–4 mice per group.

(F) Bar graph summarizing the sag at the −100 pA in ChIs of SDS mice (one-way ANOVA, $p < 0.05$).

(G) Representative action potential traces of ChIs from wild-type mice before and after a bath application of ZD7288 (15 μM).

(H and I) Summary graphs of ChI firing rate before and after a bath application of ZD7288 in control and p11 cKO mice (H, interaction, $p = 0.01$) or in SDS mice (I, interaction, $p = 0.03$). Two-way repeated-measures ANOVA. n = 7–9 cells from 3 mice per group.

Scale bar for (A) and (D), 20 mV, 100 ms; for (G), 20 pA, 1 s. Data are represented as means ± SEM. *$p < 0.05$, **$p < 0.01$.

Taken together, these data indicate a disrupted HCN function in p11 cKO mice and susceptible mice.

The regulation by HCN channels of neuronal activity depends on cellular localization. To study the regulation by HCN channels of the ChIs in the NAc, cell-attached voltage clamping was performed in the presence of ZD7288, a selective inhibitor of HCN channels. We confirmed that ZD7288 was efficient to inhibit HCN currents in ChIs (Figure S5F). Bath application of ZD7288 lead to a progressive and significant reduction in the ChI firing rate in wild-type mice (Figure 5G), suggesting a positive regulation of ChI activity by HCN channels. Blocking the HCN channel lead to similar remaining firing rates in p11 cKO mice and SDS mice compared to their control mice (Figures 5H and 5I). These data suggest that the diminished ChI firing rate observed in depressive mice is mainly caused by dysfunction of HCN channels.

Overexpression of HCN2 Rescues Depressed Mice

Based on our evidence that HCN2 channels were transcriptionally and functionally suppressed in NAc ChIs in mouse models of depression, we hypothesized that HCN2 channels are a potential antidepressant target. To selectively overexpress HCN2 in NAc ChIs, we used a Cre-dependent loxP-STOP-loxP herpes simplex virus with enhanced yellow fluorescent protein (HSV-LS1L-HCN2-eYFP) and HSV-LS1L-eYFP as control. The HSV vector allows for a rapid expression of HCN2 channels from day 3 to day 8 after stereotaxic injection (Friedman et al., 2014). The HSV viruses were injected bilaterally into the NAc of ChAT-Cre mice and were shown to be expressed in the ChIs (Figure 6A). Electrophysiological validation was performed 4 days after the virus injection. Overexpression of HCN2 induced increased HCN currents and firing rate in ChIs compared to those in control (Figures 6B and 6C).

Behavioral tests were performed to examine the rescue effects of HCN2 in depressed mice. In the SDS model, HCN2 HSV was injected into the NAc of susceptible mice and SI was performed 4 days later (Figure 6D). We found that HCN2 overexpression markedly reversed the social avoidance in susceptible mice (Figures 6E). The time that the susceptible mice spent interacting with aggressors was elevated with HCN2 overexpression (Figure 6F).

Please cite this article in press as: Cheng et al., HCN2 Channels in Cholinergic Interneurons of Nucleus Accumbens Shell Regulate Depressive Behaviors, Neuron (2018), https://doi.org/10.1016/j.neuron.2018.12.018

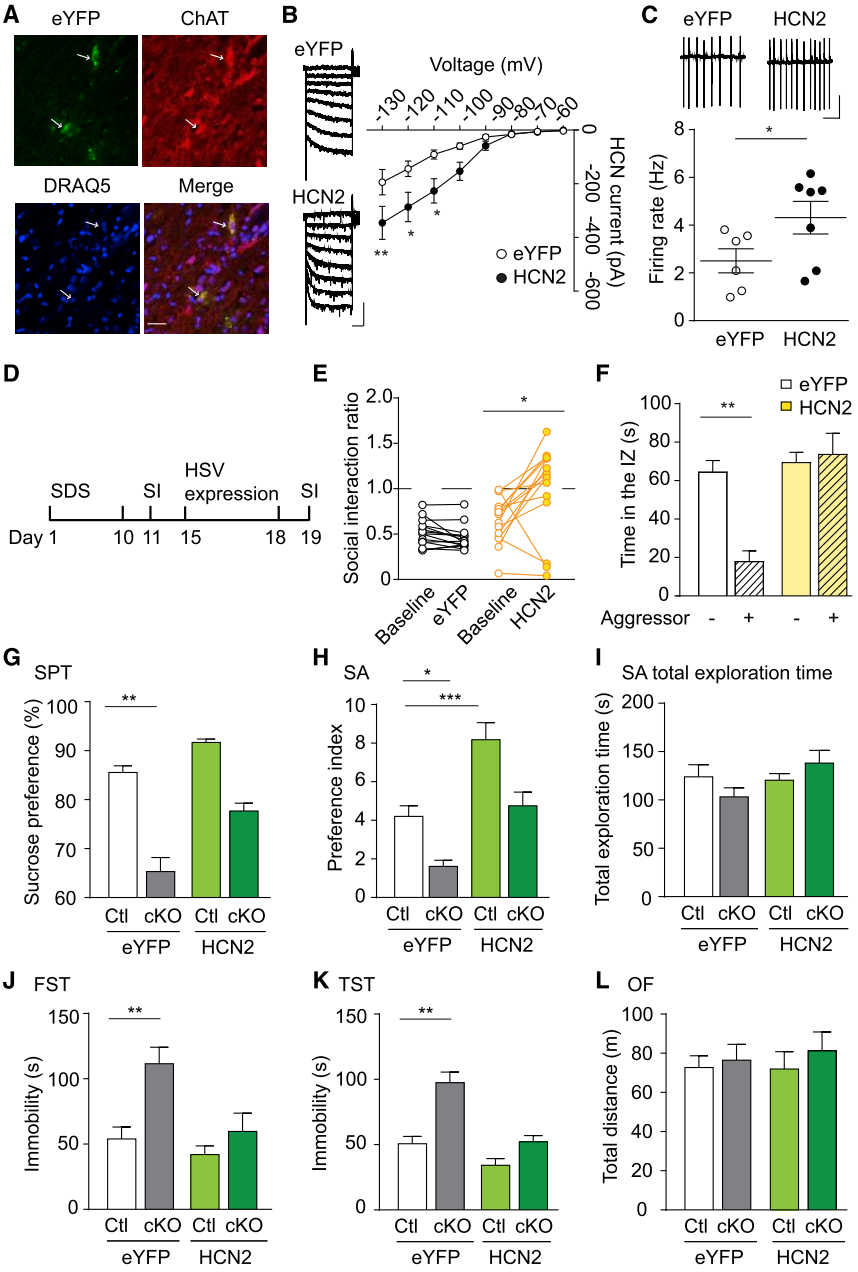

Figure 6. ChI-Specific Overexpression of HCN2 Channels Exerts Antidepressant Effects

(A) Representative confocal images showing the expression of HCN2 HSV (eYFP, green), cholinergic interneurons (ChAT, red), and DRAQ5. Arrows indicate co-localization of eYFP and ChAT in DRAQ5 positive cells. HSV-expressing ChAT$^+$ neurons are 45.0% ± 5.0% of total ChAT$^+$ neurons in the NAc. No HSV is expressed in the ChAT$^-$ neurons (2–3 sections per mouse; n = 3 mice). Scale bar, 20 μm.

(B) Representative traces and current-voltage curve of HCN currents in ChIs expressing eYFP HSV or HCN2 HSV (two-way ANOVA, interaction, $p < 0.05$; virus, $p < 0.001$; voltage, $p < 0.001$). n = 8 cells from 3 mice per group. Scale bar, 200 pA, 750 ms.

(C) Representative traces and summary plot of ChI firing rate (unpaired t test). n = 6–7 cells from 3 mice per group. Scale bar, 20 pA, 1 s.

(D) Timeline of experimental design.

(E) SI ratio of susceptible mice before and after the expression of eYFP or HCN2 HSV (one-way repeated-measures ANOVA, $p < 0.001$). n = 15 mice per group.

(F) Time spent in the interaction zone by susceptible mice expressing eYFP or HCN2 HSV in the absence or presence of aggressors (two-way repeated-measures ANOVA, interaction, $p < 0.001$).

(G–L) Behavioral tests of control and p11 cKO mice expressing eYFP or HCN2 HSV. Two-way ANOVA. n = 8–12 mice per group.

(G) Sucrose preference test (interaction, p = 0.11; genotype, $p < 0.001$; HSV, $p < 0.001$).

(H) Social approach preference index (interaction, p = 0.54; genotype, $p < 0.001$; HSV, $p < 0.001$).

(I) Total exploration time in social approach test (interaction, p = 0.06; genotype, p = 0.90; HSV, p = 0.10).

(J) Forced swim test (interaction, $p < 0.05$; genotype, $p < 0.01$; HSV, $p < 0.01$).

(K) Tail suspension test (interaction, $p < 0.05$; genotype, $p < 0.01$; HSV, $p < 0.01$).

(L) Open-field test (interaction, p = 0.74; genotype, p = 0.43; HSV, p = 0.81).

All data are presented as means ± SEM. *$p < 0.05$, **$p < 0.01$, ***$p < 0.001$.

See also Figure S6.

SPT was further performed to show that depressive phenotypes in susceptible mice were rescued by HCN2 HSV (Figure S6A). We next examined behavioral consequences of HCN2 HSV in p11 cKO mice. Overexpression of HCN2 by HSV enhanced sucrose consumption and SI and reduced immobility in the FST and TST without affecting locomotion in p11 cKO mice (Figures 6G–6L). In line with Gs DREADD, overexpression of HCN2 in control mice was efficient to modulate sucrose consumption and SI, supporting that ChI activity plays a central role in controlling reward response and sociability (Figures 6G and 6H).

Although HSV has been widely used, there are potential post-surgery effects on mouse behaviors due to a short recovery time. To circumvent this possibility, we generated AAV-FLEX-HCN2 virus, which was shown to increase HCN currents in NAc ChIs (Figure S6B). Behavioral tests were performed in animals 3 weeks after stereotaxic injection of HCN2 AAV. Immunostaining confirmed a selective expression of HCN2 AAV in the NAc (Figure S6C). Consistent with the HCN2 HSV, overexpression of HCN2 in NAc ChIs reversed the anhedonia and behavioral despair in the p11 cKO mice (Figures S6D–S6I). Taken together, these data suggest that enhancing HCN2 expression in the NAc ChIs sufficiently and effectively rescues depression-like behaviors in mouse models of depression.

DISCUSSION

Common Features for Stress-Induced and Genetic Animal Models of Depression

Animal models of depression play an essential role in the study of the pathophysiology of depression. Each model exhibits distinct features (Akil et al., 2018). SDS is a commonly used animal model to investigate both the pathophysiology of depression and the action of chronic treatments since the behavioral abnormalities in the SDS mice last for weeks (Berton et al., 2006). Chronic RS, on the other hand, induces short- but not long-lasting depressive phenotypes in rodents, which is suitable only for the study of the pathophysiology of depression. A previously reported genetic mouse model of depression, p11 cKO mice (Warner-Schmidt et al., 2012), was used in the current study. p11 (S100A10), a small adaptor protein, is decreased at the mRNA and protein levels in the anterior cingulate cortex and the NAc in depressed individuals (Svenningsson et al., 2006). In addition, selective removal of p11 from the NAc ChIs in wild-type mice is sufficient to induce depressive phenotypes, whereas selective overexpression of p11 in the NAc ChIs reverses the depressive behaviors in the p11 constitutive KO mice (Warner-Schmidt et al., 2012). p11 interacts with the serotonin receptors including 5-HT1B receptor, 5-HT1D receptor, and 5-HT4 receptor (Svenningsson et al., 2006; Warner-Schmidt et al., 2009). Recent studies suggest that the interaction between p11 and 5-HT1B receptor in the cholecystokinin (CCK) cells in ventral hippocampus is relevant for the antidepressant response (Medrihan et al., 2017). The precise regulation of serotonin receptors by p11 in depression and antidepressant actions remains to be fully studied.

Here, we revealed that a reduced activity of ChIs in the NAc shell is a common feature for two stress mouse models and a genetic mouse model of depression. Our data strongly suggest that chronic stress and p11 signaling converge on the same molecular target, HCN2 channel, in NAc ChIs. However, the underlying mechanisms of the diminished HCN expression and function may be different between the stressed mice and p11 cKO mice. In the p11 cKO mice, HCN function and ChI activity are reduced in both NAc shell and core, suggesting a regulation of HCN transcription by a p11-dependent signaling pathway. However, in the stress mouse models, the HCN function and ChI activity are selectively reduced in NAc shell, but not core, which may result from distinct circuit regulation or different protein expression profiles. Since the anatomical, functional, and circuit characteristics of ChIs between shell and core are unknown, future studies are necessary in order to elucidate these differences.

NAc ChIs in the Pathophysiology of Depression

According to the Diagnostic and Statistical Manual of Mental Disorders (DSM), 5th Edition, core symptoms of depression include depressed mood and loss of interest or pleasure (anhedonia). In rodents, depression-like behaviors are subdivided into seven categories including anhedonia, reduced SI, and despair (Sukoff Rizzo and Crawley, 2017). The SPT and the SA test are the commonly used measures of reward response and sociability, respectively (Russo and Nestler, 2013). We found that acute modulation of NAc ChI activity bi-directionally regulates sucrose consumption and SI in mice, suggesting that NAc ChIs play a dominant role in controlling reward response and sociability. These findings are consistent with a previous study showing that the synaptic modifications in the D1 medium spiny neurons (MSNs) in the NAc are selectively associated with anhedonia, but not behavioral despair (Lim et al., 2012). Other evidence shows that orexin in NAc enhances sucrose "liking," while inhibition of acetylcholine in NAc shell reduces sucrose "liking" (Castro et al., 2016). For behavioral despair, modulation of NAc ChIs has no effects in wild-type mice but is sufficient to reverse the deficits in depressive mice, suggesting that NAc ChIs regulate behavioral despair through a circuit mechanism. Together, results from our study support the idea that distinct cellular and circuit mechanisms underlie different aspects of depressive behaviors.

HCN2 Channels as a Novel Antidepressant Target

HCN currents are critical in generating the tonic firing of ChIs (Bennett et al., 2000). However, the specific HCN isoform expressed in the NAc ChIs was unknown previously. Four isoforms of HCN channels (HCN 1–4) are expressed in the CNS with distinct expression patterns (Notomi and Shigemoto, 2004; Postea and Biel, 2011; Santoro et al., 2000). By using BacTRAP profiling and immunohistochemistry, we reveal that HCN2 is the predominant isoform expressed in the NAc ChIs, while HCN1, 3, and 4 are expressed at lower levels.

The regulation by HCN channels of animal behaviors depends on channel subunits, subcellular localization, cell types, and brain regions. HCN1 and HCN2 are the major subunits predominantly expressed in the distal dendrites of pyramidal neurons in the prefrontal cortex and hippocampus (Magee, 1999; Nolan et al., 2004; Shin and Chetkovich, 2007; Wang et al., 2007). The function of HCN channels in the dendritic spines is to weaken network inputs leading to decreased firing rates in pyramidal neurons (Arnsten 2009; Lewis et al., 2011). In contrast, HCN2 is the major subunit expressed in dopamine neurons (DA) of the ventral tegmental area (VTA) and in ChIs of the dorsal striatum. The role of HCN2 in these cell types is to enhance neuronal activity (Bennett et al., 2000; Friedman et al., 2014; Notomi and Shigemoto, 2004; Zhong et al., 2018). Overexpression of HCN2 in the VTA DA cells was recently shown to reverse behavioral deficits in depressive mice (Friedman et al., 2014; Zhong et al., 2018). Previous electrophysiology studies indicate that HCN currents regulate spontaneous firing of ChIs. Inhibition of HCN currents significantly reduces ChI firing rate (Bennett et al., 2000). Here, we confirm the positive regulation by HCN on ChI activity and further reveal that HCN2 in the NAc ChIs is associated with antidepressant effects.

Furthermore, emerging studies suggest that the Rab8b interacting protein (TRIP8b), an HCN binding protein, regulates HCN channel trafficking and is a potential therapeutic target for depression (Lewis et al., 2011; Han et al., 2017). Interestingly, our BacTRAP profiling shows no transcript expression of TRIP8b in the NAc ChIs, indicating distinct regulatory pathways of HCN2 channels in this specific cell type. Further studies could be conducted to confirm the transcript and protein level of TRIP8b in the NAc ChIs and to elucidate distinct mechanisms underlying HCN2 regulation and trafficking in ChIs.

STAR★METHODS

Detailed methods are provided in the online version of this paper and include the following:

- KEY RESOURCES TABLE
- CONTACT FOR REAGENT AND RESOURCE SHARING
- EXPERIMENTAL MODEL AND SUBJECT DETAILS
  - Mice
- METHOD DETAILS
  - NAc slice preparation and electrophysiology
  - Stereotaxic surgery
  - Behavioral assays
  - Chronic SDS
  - Chronic restraint stress
  - SSDS
  - SPT
  - SA test
  - Open field test
  - Forced swim test
  - Tail suspension test
  - Immunohistochemistry
  - RNA-seq of TRAP samples
  - Biostatistics
  - Semiquantitative PCR
  - Virus generation
- QUANTIFICATION AND STATISTICAL ANALYSIS
- DATA AND SOFTWARE AVAILABILITY

SUPPLEMENTAL INFORMATION

Supplemental Information includes six figures and two tables and can be found with this article online at https://doi.org/10.1016/j.neuron.2018.12.018.

ACKNOWLEDGMENTS

We would like to thank J. Gresack for suggestions on behavioral studies, J. Zhang for biostatistical analysis, L. Medrihan for discussions on electrophysiology, J. Chang and T. Liebmann for their suggestions on the immunohistochemistry, E. Griggs for assistance with the graphic preparation, K. George and S. Reed for mouse line maintenance, and B. Labonté for instructions on SDS model. This work was supported by the JPB Foundation (to P.G.), the Leon Black Family Foundation (to P.G.), and the United States Army Medical Research Acquisition Activity grant W81XWH-14-0130 (to Y.S.).

AUTHOR CONTRIBUTIONS

J.C., Y.S., and P.G. designed the experiments. J.C. performed and analyzed electrophysiological recordings. J.C. and J.L. performed behavioral tasks, and J.C. analyzed data. Y.S. performed and analyzed BacTRAP profiling and prepared the AAV-FLEX-HCN2. G.U. set up the SDS mouse model. G.U. and J.C. conducted the SDS procedure. J.C. and Y.S. performed and analyzed immunohistochemistry data. J.C., Y.S., and P.G. wrote the manuscript.

DECLARATION OF INTERESTS

The authors declare no competing interests.

Received: November 15, 2017
Revised: September 17, 2018
Accepted: December 12, 2018
Published: January 10, 2019

REFERENCES

Akil, H., Gordon, J., Hen, R., Javitch, J., Mayberg, H., McEwen, B., Meaney, M.J., and Nestler, E.J. (2018). Treatment resistant depression: a multi-scale, systems biology approach. Neurosci. Biobehav. Rev. *84*, 272–288.

Alexander, B., Warner-Schmidt, J., Eriksson, T., Tamminga, C., Arango-Lievano, M., Ghose, S., Vernov, M., Stavarache, M., Musatov, S., Flajolet, M., et al. (2010). Reversal of depressed behaviors in mice by p11 gene therapy in the nucleus accumbens. Sci. Transl. Med. *2*, 54ra76.

Arnsten, A.F. (2009). Stress signalling pathways that impair prefrontal cortex structure and function. Nat. Rev. Neurosci. *10*, 410–422.

Belmaker, R.H., and Agam, G. (2008). Major depressive disorder. N. Engl. J. Med. *358*, 55–68.

Bennett, B.D., Callaway, J.C., and Wilson, C.J. (2000). Intrinsic membrane properties underlying spontaneous tonic firing in neostriatal cholinergic interneurons. J. Neurosci. *20*, 8493–8503.

Berton, O., McClung, C.A., Dileone, R.J., Krishnan, V., Renthal, W., Russo, S.J., Graham, D., Tsankova, N.M., Bolanos, C.A., Rios, M., et al. (2006). Essential role of BDNF in the mesolimbic dopamine pathway in social defeat stress. Science *311*, 864–868.

Bobeck, E.N., Gomes, I., Pena, D., Cummings, K.A., Clem, R.L., Mezei, M., and Devi, L.A. (2017). The BigLEN-GPR171 peptide receptor system within the basolateral amygdala regulates anxiety-like behavior and contextual fear conditioning. Neuropsychopharmacology *42*, 2527–2536.

Brog, J.S., Salyapongse, A., Deutch, A.Y., and Zahm, D.S. (1993). The patterns of afferent innervation of the core and shell in the "accumbens" part of the rat ventral striatum: Immunohistochemical detection of retrogradely transported fluoro-gold. J. Comp. Neurol. *338*, 255–278.

Castro, D.C., Terry, R.A., and Berridge, K.C. (2016). Orexin in rostral hotspot of nucleus accumbens enhances sucrose 'liking' and intake but scopolamine in caudal shell shifts 'liking' toward 'disgust' and 'fear'. Neuropsychopharmacology *41*, 2101–2111.

Chan, C.S., Shigemoto, R., Mercer, J.N., and Surmeier, D.J. (2004). HCN2 and HCN1 channels govern the regularity of autonomous pacemaking and synaptic resetting in globus pallidus neurons. J. Neurosci. *24*, 9921–9932.

Chan, C.S., Glajch, K.E., Gertler, T.S., Guzman, J.N., Mercer, J.N., Lewis, A.S., Goldberg, A.B., Tkatch, T., Shigemoto, R., Fleming, S.M., et al. (2011). HCN channelopathy in external globus pallidus neurons in models of Parkinson's disease. Nat. Neurosci. *14*, 85–92.

Chaudhury, D., Walsh, J.J., Friedman, A.K., Juarez, B., Ku, S.M., Koo, J.W., Ferguson, D., Tsai, H.C., Pomeranz, L., Christoffel, D.J., et al. (2013). Rapid regulation of depression-related behaviours by control of midbrain dopamine neurons. Nature *493*, 532–536.

Cruz, F.C., Babin, K.R., Leao, R.M., Goldart, E.M., Bossert, J.M., Shaham, Y., and Hope, B.T. (2014). Role of nucleus accumbens shell neuronal ensembles in context-induced reinstatement of cocaine-seeking. J. Neurosci. *34*, 7437–7446.

Friedman, A.K., Walsh, J.J., Juarez, B., Ku, S.M., Chaudhury, D., Wang, J., Li, X., Dietz, D.M., Pan, N., Vialou, V.F., et al. (2014). Enhancing depression mechanisms in midbrain dopamine neurons achieves homeostatic resilience. Science *344*, 313–319.

Geschwind, D.H., and Flint, J. (2015). Genetics and genomics of psychiatric disease. Science *349*, 1489–1494.

Golden, S.A., Covington, H.E., 3rd, Berton, O., and Russo, S.J. (2011). A standardized protocol for repeated social defeat stress in mice. Nat. Protoc. *6*, 1183–1191.

Gomez, J.L., Bonaventura, J., Lesniak, W., Mathews, W.B., Sysa-Shah, P., Rodriguez, L.A., Ellis, R.J., Richie, C.T., Harvey, B.K., Dannals, R.F., et al. (2017). Chemogenetics revealed: DREADD occupancy and activation via converted clozapine. Science *357*, 503–507.

Han, Y., Heuermann, R.J., Lyman, K.A., Fisher, D., Ismail, Q.A., and Chetkovich, D.M. (2017). HCN-channel dendritic targeting requires bipartite

interaction with TRIP8b and regulates antidepressant-like behavioral effects. Mol. Psychiatry *22*, 458–465.

Lee, J., Finkelstein, J., Choi, J.Y., and Witten, I.B. (2016). Linking cholinergic interneurons, synaptic plasticity, and behavior during the extinction of a cocaine-context association. Neuron *90*, 1071–1085.

Lewis, A.S., Vaidya, S.P., Blaiss, C.A., Liu, Z., Stoub, T.R., Brager, D.H., Chen, X., Bender, R.A., Estep, C.M., Popov, A.B., et al. (2011). Deletion of the hyperpolarization-activated cyclic nucleotide-gated channel auxiliary subunit TRIP8b impairs hippocampal Ih localization and function and promotes antidepressant behavior in mice. J. Neurosci. *31*, 7424–7440.

Lim, B.K., Huang, K.W., Grueter, B.A., Rothwell, P.E., and Malenka, R.C. (2012). Anhedonia requires MC4R-mediated synaptic adaptations in nucleus accumbens. Nature *487*, 183–189.

Ludwig, A., Budde, T., Stieber, J., Moosmang, S., Wahl, C., Holthoff, K., Langebartels, A., Wotjak, C., Munsch, T., Zong, X., et al. (2003). Absence epilepsy and sinus dysrhythmia in mice lacking the pacemaker channel HCN2. EMBO J. *22*, 216–224.

Magee, J.C. (1999). Dendritic Ih normalizes temporal summation in hippocampal CA1 neurons. Nat. Neurosci. *2*, 848.

Maroso, M., Szabo, G.G., Kim, H.K., Alexander, A., Bui, A.D., Lee, S.H., Lutz, B., and Soltesz, I. (2016). Cannabinoid control of learning and memory through HCN channels. Neuron *89*, 1059–1073.

Medrihan, L., Sagi, Y., Inde, Z., Krupa, O., Daniels, C., Peyrache, A., and Greengard, P. (2017). Initiation of Behavioral response to antidepressants by cholecystokinin neurons of the dentate gyrus. Neuron *95*, 564–576.

Meredith, G.E., Baldo, B.A., Andrezjewski, M.E., and Kelley, A.E. (2008). The structural basis for mapping behavior onto the ventral striatum and its subdivisions. Brain Struct. Funct. *213*, 17–27.

Moy, S.S., Nadler, J.J., Perez, A., Barbaro, R.P., Johns, J.M., Magnuson, T.R., Piven, J., and Crawley, J.N. (2004). Sociability and preference for social novelty in five inbred strains: An approach to assess autistic-like behavior in mice. Genes Brain Behav. *3*, 287–302.

Nestler, E.J., Barrot, M., DiLeone, R.J., Eisch, A.J., Gold, S.J., and Monteggia, L.M. (2002). Neurobiology of depression. Neuron *34*, 13–25.

Nolan, M.F., Malleret, G., Dudman, J.T., Buhl, D.L., Santoro, B., Gibbs, E., Vronskaya, S., Buzsáki, G., Siegelbaum, S.A., Kandel, E.R., and Morozov, A. (2004). A behavioral role for dendritic integration: HCN1 channels constrain spatial memory and plasticity at inputs to distal dendrites of CA1 pyramidal neurons. Cell *119*, 719–732.

Notomi, T., and Shigemoto, R. (2004). Immunohistochemical localization of Ih channel subunits, HCN1-4, in the rat brain. J. Comp. Neurol. *471*, 241–276.

Oh, Y.S., Gao, P., Lee, K.W., Ceglia, I., Seo, J.S., Zhang, X., Ahn, J.H., Chait, B.T., Patel, D.J., Kim, Y., and Greengard, P. (2013). SMARCA3, a chromatin-remodeling factor, is required for p11-dependent antidepressant action. Cell *152*, 831–843.

Padilla, S.L., Qiu, J., Soden, M.E., Sanz, E., Nestor, C.C., Barker, F.D., Quintana, A., Zweifel, L.S., Rønnekleiv, O.K., Kelly, M.J., and Palmiter, R.D. (2016). Agouti-related peptide neural circuits mediate adaptive behaviors in the starved state. Nat. Neurosci. *19*, 734–741.

Pontieri, F.E., Tanda, G., and Di Chiara, G. (1995). Intravenous cocaine, morphine, and amphetamine preferentially increase extracellular dopamine in the "shell" as compared with the "core" of the rat nucleus accumbens. Proc. Natl. Acad. Sci. USA *92*, 12304–12308.

Postea, O., and Biel, M. (2011). Exploring HCN channels as novel drug targets. Nat. Rev. Drug Discov. *10*, 903–914.

Ren, W., Centeno, M.V., Berger, S., Wu, Y., Na, X., Liu, X., Kondapalli, J., Apkarian, A.V., Martina, M., and Surmeier, D.J. (2016). The indirect pathway of the nucleus accumbens shell amplifies neuropathic pain. Nat. Neurosci. *19*, 220–222.

Roth, B.L. (2016). DREADDs for neuroscientists. Neuron *89*, 683–694.

Russo, S.J., and Nestler, E.J. (2013). The brain reward circuitry in mood disorders. Nat. Rev. Neurosci. *14*, 609–625.

Santoro, B., Chen, S., Luthi, A., Pavlidis, P., Shumyatsky, G.P., Tibbs, G.R., and Siegelbaum, S.A. (2000). Molecular and functional heterogeneity of hyperpolarization-activated pacemaker channels in the mouse CNS. J. Neurosci. *20*, 5264–5275.

Shin, M., and Chetkovich, D.M. (2007). Activity-dependent regulation of h channel distribution in hippocampal CA1 pyramidal neurons. J. Biol. Chem. *282*, 33168–33180.

Stouffer, M.A., Woods, C.A., Patel, J.C., Lee, C.R., Witkovsky, P., Bao, L., Machold, R.P., Jones, K.T., de Vaca, S.C., Reith, M.E., et al. (2015). Insulin enhances striatal dopamine release by activating cholinergic interneurons and thereby signals reward. Nat. Commun. *6*, 8543.

Sukoff Rizzo, S.J., and Crawley, J.N. (2017). Behavioral phenotyping assays for genetic mouse models of neurodevelopmental, neurodegenerative, and psychiatric disorders. Annu. Rev. Anim. Biosci. *5*, 371–389.

Sullivan, P.F., Neale, M.C., and Kendler, K.S. (2000). Genetic epidemiology of major depression: review and meta-analysis. Am. J. Psychiatry *157*, 1552–1562.

Svenningsson, P., Chergui, K., Rachleff, I., Flajolet, M., Zhang, X., El Yacoubi, M., Vaugeois, J.M., Nomikos, G.G., and Greengard, P. (2006). Alterations in 5-HT1B receptor function by p11 in depression-like states. Science *311*, 77–80.

Svenningsson, P., Kim, Y., Warner-Schmidt, J., Oh, Y.S., and Greengard, P. (2013). p11 and its role in depression and therapeutic responses to antidepressants. Nat. Rev. Neurosci. *14*, 673–680.

Virk, M.S., Sagi, Y., Medrihan, L., Leung, J., Kaplitt, M.G., and Greengard, P. (2016). Opposing roles for serotonin in cholinergic neurons of the ventral and dorsal striatum. Proc. Natl. Acad. Sci. USA *113*, 734–739.

Voorn, P., Vanderschuren, L.J., Groenewegen, H.J., Robbins, T.W., and Pennartz, C.M. (2004). Putting a spin on the dorsal-ventral divide of the striatum. Trends Neurosci. *27*, 468–474.

Wallace, D.L., Han, M.H., Graham, D.L., Green, T.A., Vialou, V., Iñiguez, S.D., Cao, J.L., Kirk, A., Chakravarty, S., Kumar, A., et al. (2009). CREB regulation of nucleus accumbens excitability mediates social isolation-induced behavioral deficits. Nat. Neurosci. *12*, 200–209.

Wang, M., Ramos, B.P., Paspalas, C.D., Shu, Y., Simen, A., Duque, A., Vijayraghavan, S., Brennan, A., Dudley, A., Nou, E., et al. (2007). Alpha2A-adrenoceptors strengthen working memory networks by inhibiting cAMP-HCN channel signaling in prefrontal cortex. Cell *129*, 397–410.

Warner-Schmidt, J.L., Flajolet, M., Maller, A., Chen, E.Y., Qi, H., Svenningsson, P., and Greengard, P. (2009). Role of p11 in cellular and behavioral effects of 5-HT4 receptor stimulation. J. Neurosci. *29*, 1937–1946.

Warner-Schmidt, J.L., Schmidt, E.F., Marshall, J.J., Rubin, A.J., Arango-Lievano, M., Kaplitt, M.G., Ibañez-Tallon, I., Heintz, N., and Greengard, P. (2012). Cholinergic interneurons in the nucleus accumbens regulate depression-like behavior. Proc. Natl. Acad. Sci. USA *109*, 11360–11365.

Witten, I.B., Lin, S.C., Brodsky, M., Prakash, R., Diester, I., Anikeeva, P., Gradinaru, V., Ramakrishnan, C., and Deisseroth, K. (2010). Cholinergic interneurons control local circuit activity and cocaine conditioning. Science *330*, 1677–1681.

Zhong, P., Vickstrom, C.R., Liu, X., Hu, Y., Yu, L., Yu, H.G., and Liu, Q.S. (2018). HCN2 channels in the ventral tegmental area regulate behavioral responses to chronic stress. eLife *7*, e32420.

Zhou, F.M., Wilson, C.J., and Dani, J.A. (2002). Cholinergic interneuron characteristics and nicotinic properties in the striatum. J. Neurobiol. *53*, 590–605.

STAR★METHODS

KEY RESOURCES TABLE

REAGENT or RESOURCE	SOURCE	IDENTIFIER
Antibodies		
Rabbit anti-choline acetyltransferase (1:500)	Millipore	Cat#AB143; RRID: AB_2079760
Rabbit anti-HCN2 (1:500)	Alomone Labs	Cat#APC-030; RRID: AB_2313726
Mouse anti-GFP (1:1000)	Abcam	Cat#AB1218; RRID: AB_298911
Donkey anti-rabbit IgG Alexa 568 (1:2000)	Invitrogen	Cat#A10042: RRID: AB_2534017
Goat anti-mouse IgG Alexa 488 (1:2000)	Invitrogen	Cat#A11029; RRID: AB_138404
Chemicals, Peptides, and Recombinant Proteins		
Clozapine-N-Oxide (CNO)	Sigma-Aldrich	Cat#C0832
Bicuculline methiodide	Tocris Bioscience	Cat#2503
D-AP5	Tocris Bioscience	Cat#0106
CNQX disodium salt	Tocris Bioscience	Cat#1045
Tetrodotoxin citrate (TTX)	Tocris Bioscience	Cat#1069
Fluoxetine hydrochloride	Cayman Chemical	Cat#14418
DRAQ5	Cell Signaling Technology	Cat#4084L
Tetraethylammonium chloride (TEA)	Sigma-Aldrich	Cat#T2265
ZD 7288	Tocris Bioscience	Cat#1000
Deposited Data		
RNA-Seq of TRAP samples	This paper	GEO: GSE106389
Experimental Models: Organisms/Strains		
Mouse: ChAT^{Cre}	GENSAT	GM60
Mouse: p11$^{fl/fl}$	Greengard lab	p11
Mouse: ChAT ^{bacTRAP}	GENSAT	DW167
Mouse: ChAT ^{eGFP}	GENSAT	GH293
Recombinant DNA		
rAAV2-hSyn-DIO-hM4D (Gi)-mCherry	UNC Vector Core	N/A
rAAV2-hSyn-DIO-rM3D (Gs)-mCherry	UNC Vector Core	N/A
rAAV2-hSyn-DIO-mCherry	UNC Vector Core	N/A
HSV-LS1L-HCN2-eYFP	MGH Gene Delivery Technology Core	N/A
HSV-LS1L-eYFP	MGH Gene Delivery Technology Core	N/A
rAAV2-Flex-HCN2	This paper	N/A
rAAV2-Flex-mCherry	This paper	N/A
pAAV-Flex-GFP	Addgene	28304
pAAV-Flex-HCN2	This paper	N/A
pAAV-Flex-mCherry	This paper	N/A
Software and Algorithms		
Graphpad Prism 6.0	GraphPad Software	https://www.graphpad.com/scientificsoftware/prism/
pClamp 10	Molecular Device	https://www.moleculardevices.com/products/axon-patch-clamp-system/acquisition-and-analysis-software/pclamp-software-suite
ImageJ	NIH	https://imagej.nih.gov/ij/
Illustrator CS6	Adobe	https://www.adobe.com/products/illustrator.html
Zen software	Zeiss	https://www.zeiss.com/microscopy/us/products/microscope-software/zen-lite.html
FASTQC	BBSRC, UK	https://www.bioinformatics.babraham.ac.uk/projects/fastqc/

(*Continued on next page*)

Continued

REAGENT or RESOURCE	SOURCE	IDENTIFIER
Tophat	Johns Hopkins University	http://ccb.jhu.edu/software/tophat/index.shtml
Cufflink	University of Washington	http://cole-trapnell-lab.github.io/cufflinks/
DESeq	EMBL Heidelberg, Germany	http://bioconductor.org/packages/release/bioc/html/DESeq.html
DAVID	NIAID	https://david.ncifcrf.gov/

CONTACT FOR REAGENT AND RESOURCE SHARING

Further information and requests for resources and reagents should be directed to and will be fulfilled by the Lead Contact, Dr. Paul Greengard (greengard@rockefeller.edu).

EXPERIMENTAL MODEL AND SUBJECT DETAILS

Mice

All procedures involving mice were approved by the Rockefeller University Institutional Animal Care and Use Committee and were in accordance with the National Institutes of Health Guide for the Care and Use of Laboratory Animals. Mice were maintained on a C57BL/6 background and were kept on a 12-h light/dark cycle with food and water *ad libitum*. Mice were housed in groups of up to five animals except for mice that underwent chronic SDS and chronic restraint stress, which were housed singly to avoid fighting. CD-1 male retired breeders were purchased from Charles River Laboratories. p11 cKO mice were generated as previously described (Warner-Schmidt et al., 2012; Virk et al., 2016). ChAT-Cre mice, ChAT-eGFP mice and ChAT bacTRAP mice were maintained heterozygous as described previously (Virk et al., 2016). Male mice between eight to twelve weeks of age were used for all behavioral tests. Male and female mice were used for molecular and physiological studies, with no differences observed between genders.

METHOD DETAILS

NAc slice preparation and electrophysiology

Mice were euthanized with CO_2. Their brain was quickly removed and placed in an ice-cold N-Methyl-D-glucamine (NMDG)-containing cutting solution (in mM: 93 NMDG, 2.5 KCl, 1.2 NaH_2PO_4, 30 $NaHCO_3$, 25 glucose, 20 HEPES, 5 sodium ascorbate, 3 sodium pyruvate, 2 thiourea, 0.5 $CaCl_2$, 10 $MgSO_4$, pH 7.4, 295-305 mOsm). Coronal brain slices (300 μm thickness) containing the NAc were cut by using a VT1000 S Vibratome (Leica Microsystems, Buffalo Grove, IL, USA). After cutting, slices were allowed to recover in the cutting solution saturated with 95% O_2 and 5% CO_2 for 15 min at 37°C. The slices were then transferred and incubated in the recording solution at room temperature for at least 1 hour before recording.

NAc-containing slices were placed in a perfusion chamber attached to the fixed stage of an upright BX51WI microscope (Olympus, Japan) and submerged in continuously flowing oxygenated recording solution containing the following (in mM): 125 NaCl, 25 $NaHCO_3$, 25 glucose, 2.5 KCl, 1.25 NaH_2PO_4, 2 $CaCl_2$, and 1 $MgCl_2$, pH 7.4, 295-305 mOsm. Neurons were visualized with a 40x water immersion lens and illuminated with near infrared (IR) light. Electrophysiological recordings were made with a Multiclamp 700B/Digidata1440A system (Molecular Devices, Sunnyvale, CA, USA). Patch electrodes were made by pulling TW150-4 glass capillaries (World Precision Instruments, Sarasota, FL, USA) on a PP-830 Single Stage Glass Microelectrode Puller (Narishige, East Meadow, NY, USA). The pipette resistance was typically 3-5 MΩ after filling with the internal solution (in mM: 126 K-gluconate, 10 KCl, 2 $MgSO_4$, 0.1 BAPTA, 10 HEPES, 4 ATP, 0.3 GTP and 10 phosphocreatine, pH 7.3, 290 mOsm). All electrophysiological recordings were carried out blind to the experimental conditions including genotype, drug treatments and viral infection.

Cell-attached voltage-clamp or current-clamp was used to record spontaneous action potentials of ChIs in NAc slices at 32°C. Unlike whole-cell patch clamping that disturbs the intracellular contents leading to considerable diminished firing rate of ChIs during recordings, cell-attached patch clamping was chosen to produce reliable, long-lasting and stable recording of action potentials in ChIs (Bennett et al., 2000; Virk et al., 2016). After the pipette was placed on the ChI soma, a negative pressure was applied to form a seal. When the initial seal resistance maintained between 100-200 MΩ, cell-attached current clamp was performed. When the initial seal resistance exceeded 1 GΩ, cell-attached voltage clamp was performed. All other recordings were immediately abandoned. The electrode capacitance was compensated during recording.

Whole-cell voltage-clamp was made from the soma of ChIs to measure HCN currents. HCN currents were recorded with a series of three second pulses with 10 mV command voltage steps from −130 mV to −60 mV from a holding potential at −60 mV. Tetrodotoxin (TTX, 1 μM) and tetraethylammonium chloride (TEA, 5 mM) were added in the ACSF (pH 7.4, 295-305 mOsm) to block sodium currents and potassium currents, respectively. HCN current amplitudes were calculated as the difference between the instantaneous current at the beginning of the voltage step and the steady-state current at the end of the voltage step (Han et al., 2017).

p11 cKO mice (p11 $^{fl/fl}$: ChAT-Cre $^{+/-}$) and control mice (p11 $^{fl/fl}$) were crossed with chat-eGFP mice to visualize ChIs for the study of basal firing rate and HCN currents. ChAT-eGFP mice were used for recordings in RS and SDS mice. ChAT-Cre mice expressing mCherry-AAV, eYFP-HSV, or GFP AAV were used for recordings in virus interference experiments. To study the chronic modulation of CNO on neuronal activity of DREADD+ ChIs, ChAT-Cre male mice were used. Recording was performed 24 hours after the last injection of clozapine N-oxide (CNO). To examine drug effects on ChI activity, ChIs were recorded ten minutes as baseline and then perfused with CNO (1 μM. Medrihan et al., 2017) or ZD7288 (15 μM. Nolan et al., 2004).

All data were acquired at a sampling frequency of 50 kHz, filtered at 1 kHz and analyzed using pClamp10 software (Molecular Devices).

Stereotaxic surgery

rAAV2-hSyn-DIO-mCherry, rAAV2-hSyn-DIO-rM3D(Gs)-mCherry and rAAV2-hSyn-DIO-hM4D(Gi)-mCherry viruses were purchased from the University of North Carolina vector core facility (UNC, Chapel Hill, NC, USA). HSV-LS1L-HCN2-eYFP and HSV-LS1L-eYFP were purchased from Rachael Neve in Gene Delivery Technology Core in Massachusetts General Hospital (Cambridge, MA, USA). HCN2 AAV plasmid was generated by our group and further packaged by UNC-Vector Core (UNC at Chapel Hill).

All stereotaxic surgeries were performed on an Angle Two Small Animal Stereotaxic Instrument (Leica Biosystems, Buffalo Grove, IL, USA) with a microinjection syringe pump (World Precision Instruments, Sarasota, FL, USA). Male mice (six-eight weeks of age) were anesthetized with a mix of ketamine (100 mg/ml) and xylazine (1 mg/ml). Viruses (1 μl) were injected bilaterally into the NAc shell (+ 1.6 mm anterior-posterior (AP), ± 0.8 mm medial-lateral (ML) and −4.7 dorsal-ventral (DV) from bregma) with a 10 mL Hamilton syringe at a speed of 0.1 μl/min. The needle was left for an additional 10 min and then was slowly withdrawn. The stereotaxic injections were confirmed by immunohistochemistry to adequately cover the NAc without significant spread to other regions.

Mice were monitored for 48 hours to ensure full recovery from the surgery. Experiments using AAVs were performed three weeks after stereotaxic surgery allowing the fully expression of viruses. For the HCN2 HSV experiments, behavioral tests, immunohistochemistry and electrophysiological recordings were performed four to seven days post-surgery.

Behavioral assays

All the behavioral tests were performed and analyzed by experimenters blinded to the genotype of animals and drug treatments. Cohorts of mice undergoing multiple tests were testified in the following order: SPT, SA test, open field test (OF), forced swim test (FST) and tail suspension test (TST), with at least 24 hour of interval between tests. For chemogenetic experiments, CNO (1 mg/kg, Padilla et al., 2016; Bobeck et al., 2017) or saline were intraperitoneally (i.p.) injected into the mice 1 hour before the start of behavioral tests.

Chronic SDS

The chronic SDS was carried out as described previously (Golden et al., 2011). 3-month-old retired male breeder CD-1 mice were screened over three consecutive days and aggressors were selected according to the following criteria: (i) the latency to the initial attack was under 60 s and (ii) the screener mouse was attacked for 2 consecutive days. For ten consecutive days, the experimental mice were placed in the home cage of a prescreened CD-1 aggressor for a 5-min physical attack and then separated by a perforated divider for the remaining 24 hours until the next defeat. Each day, the aggressors were exposed with a different experimental mouse. In parallel, control mice (stress-naive ChAT-eGFP mice for electrophysiology and stress-naive ChAT-Cre mice for behaviors) were placed in pairs within an identical home cage setup separated by a perforated divider for the duration of the defeat sessions. They were never in physical or sensory contact with CD-1 mice.

After 10 days of SDS, all aggressors and experimental mice were separated and singly housed. The SI test was performed 24 hr later. SI test was composed of two phases where the experimental mice were allowed to explore an open field (42 cm x 42 cm x 42 cm) with a wire mesh enclosure (10 cm wide x 6.5 cm deep x 42 cm high). In the first phase, the wire mesh enclosure was empty. In the second phase, a novel CD-1 aggressor mouse was placed inside the wire mesh. The amount of time the experimental mice spent in the interaction zone (IZ) surrounding the wire mesh enclosure was collected and analyzed by the video-tracking apparatus and software EthoVision XT (Noldus Information Technology, Leesburg, VA, USA). SI ratio was calculated by dividing the amount of time the experimental mice spent in the IZ in phase two over the time in phase one. Susceptible mice were defined by a SI ratio under 1 and an interaction time in phase two less than 60 s whereas resilient mice were defined by a SI ratio greater than 1 and the interaction time in phase two more than 60 s.

Chronic restraint stress

The chronic restraint stress (RS) paradigm was modified according to previous studies (Oh et al., 2013). Briefly, eight-week-old male mice were individually placed into well-ventilated 50 mL polypropylene conical tubes, which were then plugged with a 4.5-cm-long middle tube and tied with the cap of the 50 mL tube. The restraint stress lasted 4 hours per day (9:00 am to 1:00 pm) for 21 days. Mice were returned to their home cages after restraint session each day, where they were housed with free access to food and water. Control mice were housed in the same room with no exposure to stressor. ChAT-eGFP mice underwent RS for electrophysiological recordings while wild-type C57BL/6 mice underwent RS for behavioral tests. All experiments were performed 24 hour after the termination of the RS.

SSDS

The subthreshold social defeat stress (SSDS) was performed as described previously (Golden et al., 2011). mCherry or Gi-DREADD AAV was injected into the NAc of ChAT-Cre male mice at 6 weeks of age. Three weeks post-surgery, virus was fully expressed in NAc ChIs. Mice were injected with a single dose of CNO and then subjected to the SSDS one hour later. The activity of ChIs was inhibited during the defeat episodes. In the SSDS, experimental mice were placed into the home cage of a CD-1 aggressor for a 5-min physical defeat. Mice were then allowed to rest in their home cage for 15 min. Defeat episodes were repeated twice. After SSDS, experimental mice were returned to their home cage. Behavioral tests were performed 24 hour after the SSDS with no additional treatment of CNO.

SPT

In the home cage, mice were habituated with two identical water bottles for 24 hour. One water bottle was then replaced with 1.5% sucrose solution. Bottle locations were randomly assigned and flipped at 12 hour to prevent potential preference in side. The consumption of water and sucrose solution was measured 24 hour later by weighing the bottles. The sucrose preference was calculated as $(\Delta\text{weight}_{\text{sucrose}}) / (\Delta\text{weight}_{\text{sucrose}} + \Delta\text{weight}_{\text{water}}) \times 100\%$.

SA test

The SA test was adapted from previous studies (Moy et al., 2004). The apparatus was a rectangular, three-chambered box. Each chambers was 20 cm × 40.5 cm × 22 cm. Two retractable doorways in the apparatus allowed for access to each chambers. One wire cup was placed in the left chamber and one in the right chamber, with an upright plastic drinking cup on top to prevent experimental mice from climbing up.

The SA test was composed of two 10-min phases. In phase one, experimental mice were first placed in the middle chamber and allowed to explore the apparatus with empty wire cups. In phase two, a novel object such as Lego was placed in the wire cup in one chamber. A novel conspecific that had no prior contact with the experimental mice was placed in the wire cup in the other side chambers. For the SA tests of SDS mice, a novel CD-1 aggressor was used. To prevent a possible bias, the location of novel mouse and object was alternated between trials. Animals were video recorded. The time spent in each chamber that the experimental mice approaching novel mouse or novel object was recorded and quantified by an experimenter blinded to the identity of the mice. SA preference index was calculated by dividing the amount of time the experimental mice spent approaching the novel mouse by the time spent approaching the novel object. Total exploration time was calculated by adding the amount of time the experimental mice spent approaching the novel mouse and the novel object.

Open field test

Mice were habituated in the test room for 60 min in their home cages. Locomotor activity was assayed in a square arena (50 cm x 50 cm x 22.5 cm) with two rows of infrared photocells placed 20 mm and 50 mm above the floor. Total distance traveled during a 60 min test session was automatically recorded and calculated by using the automated Superflex software (Accuscan Instruments, Columbus, OH, USA).

Forced swim test

Mice were individually placed into a glass cylinder (15cm diameter, 35cm height) filled with water (23 ± 1°C) to a height of 15 cm. Test sessions lasted 6 min and were video recorded. The duration of behavioral immobility was measured by using an automated TST/FST analysis software (Clever System, Reston, VA, USA). The amount of time spent immobile in the last 4 min of the test session was analyzed.

Tail suspension test

Mice were suspended by the tail from a horizontal bar (35 cm above the floor) using adhesive tape applied 1 cm from the tip of the tail. The test session was videotaped for 6 min and the immobility was analyzed during the last 4 min by using the automated TST/FST analysis software.

Immunohistochemistry

Mice were transcardially perfused with 4% paraformaldehyde in PBS and post-fixed at 4°C overnight. Brains were equilibrated in 30% sucrose solution and then sectioned (40 μm) using a cryostat (Leica Biosystems, Wetzlar, Germany). Slices were subjected to free-floating immunohistochemistry by using standard procedures. Briefly, sections were washed in PBS and blocked with 0.2% Triton X-100 and 5% normal goat serum (NGS) for 1 hour at room temperature. Then, slices were incubated with primary antibodies overnight at 4°C, washed at room temperature three times in PBS before incubation for 1 hour with Alexa Fluor-conjugated secondary antibodies (Invitrogen, Carlsbad, CA, USA). To co-stain with DRAQ5, slices were washed three times in PBS and then incubated with PBS containing DRAQ5 dye (5 mM) for 10 minutes at room temperature. Slices were washed with PBS and slide mounted. Antibodies used here were as follows: rabbit anti-choline acetyltransferase (1:500; Millipore, Billerica, MA, USA), rabbit anti-HCN2 (1:500; Alomone, Israel), rabbit anti-HCN2 (1:500; Cell signaling, Danvers, MA), Mouse anti-GFP (1:1000; Abcam, Cambridge, MA), Donkey anti-rabbit IgG Alexa 568 (1:2000; Invitrogen) and Goat anti-mouse IgG Alexa 488 (1:2000; Invitrogen). Images were taken using a LSM710 confocal microscope (Zeiss, Germany).

RNA-seq of TRAP samples

6 striata from 3 ChAT bacTRAP mice were pooled for one translating ribosome affinity purification sample. The quantity and quality of all RNA samples were validated by Bioanalyzer RNA 6000 pico kit (Agilent, San Diego, CA). For global transcript analysis, 1 ng of RNA from each I.P. sample was reversed transcribed using Ovation RNA-seq V2 kit (Nugen, San Carlos, CA). 150 bp long, single end labeled cDNA libraries were constructed using Truseq RNA sample preparation kit V2 (Illumina, San Diego, CA) and were sequenced by Illumina HiSeq 2500 Sequencer.

Biostatistics

The raw sequencing files were aligned to the *Mus musculus* genome mm10 using Tophat (version 2.0.8). The parameter setting for Tophat was: -g 1–no-coverage-search -G genes.gtf. The data source for the reference genome mm10 and the genes.gtf file was UCSC. After alignment, the fragments per kilobase of transcript per million mapped reads (FPKM) values of genes were calculated with Cufflinks (version 2.1.1). The parameter setting for Cufflinks was: -G genes.gtf. The genes.gtf file was the same as the one used for Tophat. The differential gene expression testing between WT and p11 cKO was conducted with DESeq package (version 1.10.1) with the standard comparison mode between two experimental conditions. For biological clustering to identify enriched ontologies, the Database for Annotation, Visualization and Integrated Discovery (version 6.8) was used. These data have been deposited in NCBI's Gene Expression Omnibus and are accessible through the accession number GSE106389.

Semiquantitative PCR

For semiquantitative PCR (qPCR) analysis, 1 ng of RNA was reverse transcribed using Ovation PicoSL WTA System V2 kit (Nugen Technologies), and 20 ng of cDNA was used as a template for analysis. TaqMan Gene Expression Assays and Taqman Universal PCR Master Mix, no AmpErase UNG (Life Technologies) was used for all analyses. Fluorescence was detected using ABI 7900HT (Applied Biosystems).

Virus generation

rAAV2-Flex-HCN2 and rAAV2-Flex-mCherry were made by sub-cloning their sequences into pAAV-Flex-GFP. rAAV packaging was done at the UNC GTC Vector Core facility with respective titers of $1X10^{12}$ and $3X10^{12}$ virus molecules per ml.

QUANTIFICATION AND STATISTICAL ANALYSIS

Data ware presented as mean ± SEM except qPCR data that was presented as mean ± SD. Sample sizes and statistical methods of each experiment were provided in corresponding figure legends. For electrophysiology studies, n represented neurons; for behavioral tests and immunohistochemistry, n represented mice; for RNA-Seq and qPCR, n represented biological replicates. Statistics were analyzed by using GraphPad Prism 6 (GraphPad Software, La Jolla, CA, USA). D'Agostino-Pearson omnibus normality test was performed to test the normal distribution of all data. Group means were compared by Student's unpaired t test, Student's paired t test, one-way ANOVA, two-way ANOVA, one-way repeated-measures ANOVA, two-way repeated-measures ANOVA followed by Bonferroni post hoc test where appropriate. Correlation was analyzed by using Pearson correlation. Enriched genes from the RNaseq experiment were determined using Student's unpaired t test, followed by the false discovery rate (FDR) with the Benjamini-Hochberg procedure to adjust for multiple comparisons. pClamp 10 (Molecular Devices) was used to analyze electrophysiological data. Statistical significance is shown as * $p < 0.05$, ** $p < 0.01$, *** $p < 0.001$.

DATA AND SOFTWARE AVAILABILITY

The accession number for the raw files for the RNA-Seq experiment reported in this paper is GEO: GSE106389. Data generated in this study will be provided upon request to the Lead Contact, Paul Greengard (greengard@rockefeller.edu).